Arch Iran Med. March 2026;29(3):133-147

doi:10.34172/aim.35172

http://journalaim.com

ARCHIVES OF IRANIAN MEDICINE

Original Article

Open Access

Patterns and Temporal Dynamics of Pediatric Solid Malignant Tumors: Insights from a 27-Year Referral Center Cohort in Iran (1996–2022)

Maryam Kazemi Aghdam[1], Yalda Nilipour[1,2], Seiedehparnian Taghvaei[1], Bibi Shahin Shamsian[3], Samin Alavi[3], Nader Momtazmanesh[4], Peyman Eshghi[3], Gholamreza Ebrahimisaraj[5,6*], Mehdi Sarafi[5], Leili Mohajerzadeh[5], Javad Ghoroubi[5], Mohsen Rouzrokh[5], Ahmad Khaleghnejad Tabari[5]

[1]Pediatric Pathology Research Center, Research Institute for Children's Health, Shahid Beheshti University of Medical Sciences, Tehran, Iran
[2]Neuromuscular Research Center, Tehran University of Medical Sciences, Tehran, Iran
[3]Pediatric Congenital Hematologic Disorders Research Center, Research Institute for Children's Health, Shahid Beheshti University of Medical Sciences, Tehran, Iran
[4]Department of Pediatric Hematology and Oncology, Mofid Children Hospital, Shahid Beheshti University of Medical Sciences, Tehran, Iran
[5]Pediatric Surgery Research Center, Research Institute for Children's Health, Shahid Beheshti University of Medical Sciences, Tehran, Iran
[6]Department of Pediatric Surgery, Pediatric Surgery Research Center, Mofid Children's Hospital, Shahid Beheshti University of Medical Sciences, Tehran, Iran

Abstract

Introduction: Pediatric solid malignant tumors cause a growing concern with regional variations. Long-term data from Iran are limited. This study examined the temporal trends and distribution of these tumors over 27 years in a large referral cohort, focusing on patterns rather than absolute national incidence.

Methods: We retrospectively analyzed 2,579 children diagnosed with solid malignant tumors at Mofid Children's Hospital, Tehran (1996–2022). Demographics, tumor types, and temporal patterns were assessed. Joinpoint regression evaluated temporal trends using population-standardized and crude rates as analytic denominators for trend assessment. Age–Period–Cohort models were fitted for lymphomas, central nervous system (CNS), and sympathetic nervous system (SNS) tumors. Age-standardized incidence rates (ASIRs) and incidence rate ratios (IRRs) were calculated.

Results: Children aged 1-4 years predominated (45.1%). CNS and SNS tumors were most common (40.8%), followed by lymphomas (16.7%). Referral-based population-standardized diagnosis rates increased significantly over time (1996–2022; AAPC = 4.81%, $P < 0.001$), with similar trends for crude rates (AAPC = 6.03%, $P < 0.001$). CNS and SNS tumors showed the steepest and most consistent increases. Age–period–cohort analyses indicated dominant calendar period effects, particularly for CNS and SNS tumors, while age effects were tumor-specific and cohort patterns were variable. Incidence rate ratios demonstrated higher referral-based diagnosis rates in 2014–2022 across all age groups, most pronounced for CNS and SNS tumors in younger children. Tumor composition shifted over time, with increasing CNS and SNS contributions.

Conclusion: Over 27 years, referral-based pediatric solid tumor diagnoses increased significantly, driven by CNS and SNS tumors. Our findings underscore complex temporal dynamics in referral-based pediatric solid tumor diagnoses and highlight the need for enhanced surveillance and etiologic research.

Keywords: Cohort analysis, Lymphoma, Neoplasms, Pediatric, Trend analysis

Cite this article as: Kazemi Aghdam M, Nilipour Y, Taghvaei SP, Shamsian BS, Alavi S, Momtazmanesh N, et al. Patterns and temporal dynamics of pediatric solid malignant tumors: insights from a 27-year referral center cohort in Iran (1996–2022). Arch Iran Med 2026;29(3):133-147. doi:10.34172/aim.35172

Received: September 26, 2025, **Revised:** December 15, 2025, **Revised:** January 5, 2026, **Accepted:** February 10, 2026, **ePublished:** March 1, 2026

Introduction

Pediatric cancer continues to be a major public health issue across the globe, ranking among the top causes of death from illness in both children and teenagers.[1,2] Global Cancer Observatory data from 2022 indicates a significant burden of pediatric cancer among children aged 0 to 14. Over 200,000 new cancer diagnoses were recorded in this age group, with cases notably higher in boys (approximately 114,000) than girls (around 87,000). In the same year, approximately 77,000 deaths were attributed to cancer within this young demographic; fatalities among boys totaled about 44,000, while girls accounted for roughly 33,000 deaths.[3,4] While significant advancements in diagnosis and treatment have led to remarkable improvements in survival rates, reaching over 80% in high-income countries, a stark disparity persists in low- and middle-income regions, where survival rates can be as low as 20%.[5,6] This underscores the critical need

*Corresponding Author: Gholamreza Ebrahimisaraj, Emails: gh.saraj@sbmu.ac.ir; gh.saraj@gmail.com

for comprehensive epidemiological data, particularly in diverse geographical settings, to inform targeted interventions and resource allocation.

Among pediatric malignancies, solid tumors constitute a substantial proportion, accounting for approximately 60–70% of all childhood cancers, distinct from hematologic neoplasms in their clinical features and cellular origins.[7,8] Understanding the specific incidence patterns, demographic characteristics, and temporal trends of these tumors is crucial for public health planning, cancer control programs, and clinical management.

The reported age-standardized incidence rate (ASIR) for all childhood cancers in Iran is approximately 120 per 1 million individuals, with considerable variations across geographical regions and between sexes.[9,10] While leukemia generally represents the most common childhood cancer, solid tumors of the brain and nervous system, lymphomas, bone, and connective and soft tissue are also prevalent.[9] However, detailed, long-term, single-center epidemiological studies focusing specifically on solid malignant tumors in a major pediatric referral center can provide invaluable granular insight into local disease burden and evolving patterns.

Building upon a previous investigation conducted at the same institution ("Survey on Childhood Solid Malignant Tumors in Cases Admitted to Mofid Pediatric Hospital From 1996–2010: A Single-Center Study," published in *Iran J Cancer Prev* 2012; 2:93–104),[11] the present study aims to provide a more comprehensive and updated understanding of these malignancies over an extended 27-year period. Unlike the earlier descriptive analysis, this study employs robust statistical methods—including Age-Period-Cohort modeling, age-standardized incidence rates (ASIRs), Annual Percent Change (APC), and Incidence Rate Ratios (IRRs)—using population denominators as analytical references to assess longitudinal temporal trends, rather than to estimate national incidence. Importantly, our primary objective was not to establish countrywide incidence rates, but rather to investigate temporal trends in tumor distribution, diagnosis patterns, and clinical characteristics within this large single-center cohort. By focusing on patterns and changes over time, this study provides insight into the evolving epidemiology of pediatric solid malignancies in Iran. Given Mofid Pediatric Hospital's status as a major national referral center, the findings may reflect broader national temporal patterns, while remaining inherently referral-based.

Patients and Methods

Study Design and Setting

This investigation was designed as a descriptive, retrospective, single-center referral-based study, evaluating temporal patterns and referral-based occurrence of solid malignant tumors in children and adolescents. The study was conducted at Mofid Pediatric Hospital, one of Iran's largest pediatric referral centers, encompassing a comprehensive period from January 1996 to December 2022. Because this study was a retrospective analysis of all pediatric solid malignant tumors diagnosed at the national referral pediatric oncology center from 1996–2022, no *a-priori* sample size calculation was performed. Instead, the sample size (n = 2,579) represents the complete population of eligible cases captured over the 27-year period, thereby maximizing statistical power for temporal trend analyses of referral-based tumor occurrence.

Approval for the research design was obtained from the Institutional Review Board and the Ethics Committee affiliated with Mofid Children's Hospital, following a thorough evaluation process. As the study was conducted retrospectively and relied solely on de-identified patient records, obtaining informed consent from individual participants was deemed unnecessary and formally exempted. To uphold patient privacy, all personal identifiers were removed from the data before any analysis, thereby safeguarding confidentiality throughout the research process.

Patient Population and Eligibility Criteria

The study population comprised all pediatric and adolescent patients, aged 0–14 years, who were referred to Mofid Pediatric Hospital and diagnosed with solid malignant tumors during the specified study period. Inclusion criteria mandated a histopathological confirmation of a solid malignant tumor, independently verified by two expert pediatric pathologists. In instances where initial diagnosis remained uncertain, supplementary immunohistochemistry (IHC) assays were performed to achieve definitive diagnostic clarity.

Data Collection and Variables

Given the absence of a pre-existing comprehensive hospital-based cancer registration system prior to this study, a dedicated pediatric cancer registry was meticulously established. This involved an extensive retrospective review of patients' medical records from the hospital archives. The collected data for each eligible patient included: patient name, tissue block number, hospital admission code, age at diagnosis, assigned age group, gender, precise date of diagnosis, classification according to International Classification of Childhood Cancers (ICCC) diagnostic groups, specific tumor type, and primary tumor site.

Tumor Classification

All solid malignant tumors included in this study were systematically classified according to the International Classification of Childhood Cancers (ICCC) diagnostic categories. The ICCC is a standardized system that categorizes pediatric cancer types primarily based on histological features, aligning with the World Health Organization (WHO) classification of pediatric tumors and the International Classification of Diseases for Oncology (ICD-O). The specific ICCC diagnostic categories considered in this study were: I) lymphomas and reticuloendothelial neoplasm, II) Central Nervous System

(CNS) and miscellaneous intracranial and intraspinal neoplasm, III) Sympathetic Nervous System tumor (SNS tumors), IV) soft-tissue sarcoma, V) renal tumors, VI) germ-cell, trophoblastic and other gonadal neoplasm, VI) hepatic tumors, VIII) malignant bone tumors, and IX) other cancers and miscellaneous categories.

To ensure consistency with the ICCC criteria across the entire study period, particularly for cases diagnosed before the year 2000 when ICCC was less widely implemented, two experienced pediatric pathologists independently reviewed the original pathological slides and associated data. Necessary modifications and reclassifications were implemented to ensure adherence to the updated ICCC guidelines.

Exclusion Criteria and Data Quality Control

A rigorous data quality control process was implemented to enhance the reliability of the findings. Patients older than 14 years at the time of diagnosis were excluded, primarily due to hospital insurance policies that did not cover this age group, which could lead to a significant underestimation if included. Manual checks for duplicate records were meticulously performed by cross-referencing patient names, age, gender, date of diagnosis, and tumor type. All duplicate cases, whether arising from recurrence or routine follow-up visits, were carefully identified and excluded from the final dataset to ensure each patient was counted only once. Furthermore, any patient records with substantial missing data or an uncertain diagnosis, even after supplementary investigations, were also excluded from the analysis.

Statistical Analysis

All statistical analyses were performed using R (version 4.4.3) and GraphPad Prism (version 10.4). Descriptive statistics, including frequencies and percentages, were used to summarize demographic characteristics and referral-based tumor distributions. Associations between categorical variables were assessed using the Chi-square test when all expected cell counts were ≥ 5; otherwise, Fisher's exact test was used when expected frequencies in any cell were < 5.

Referral-Based Age-Standardized Incidence Rate (ASIR) Calculation

Annual referral-based ASIRs were calculated for each tumor type (lymphoma, CNS, and SNS) to describe temporal trends in referral-based tumor occurrence while accounting for changes in the age distribution of the national pediatric population over the 27-year study period (1996–2022). Referral-based rates were calculated using the direct standardization method. The rates were standardized using the WHO 2000–2025 standard population for ages 0–14 years.

Age-specific person-years at risk were derived from mid-year national pediatric population estimates for each calendar year, without interpolation across years. Age-specific rates were calculated as raw observed rates (cases per person-year) within each age group and calendar year; no smoothing procedures were applied to age-specific rates prior to standardization.

The ASIR for each tumor type T in year Y was calculated as:

$$ASIR_{T,Y} = \sum_{a} r_{a,Y} . w_a$$

where $r_{a,Y}$ is the observed age-specific referral-based rate in age group a in year Y, and w_a is the corresponding weight from the WHO standard population. The final ASIR values were calculated directly, without log transformation. Ninety-five percent confidence intervals (95% CIs) were estimated assuming a Poisson distribution for the observed case counts.

Because this study is based on a single tertiary referral center rather than a population-based cancer registry, the calculated ASIRs should be interpreted as referral-based population-standardized rates intended for temporal comparison rather than true population incidence rates.

Joinpoint Regression Analysis

Temporal trends in referral-based age-standardized and crude population-standardized rates of pediatric solid malignant tumors were evaluated using the Joinpoint Regression Program version 5.4.1 (National Cancer Institute, USA). The analysis modeled the natural logarithm of annual referral-based rates as the dependent variable ($\ln(\text{rate}) = xb$), with a log-linear model and Poisson variance structure, which is the recommended setting for rate data.

To address common technical issues in time-series cancer data: (A) Heteroscedasticity was accounted for using the program's weighted least squares option, which assigns weights based on the variance of each annual rate, correcting for differing variances across years; (B) Autocorrelation was adjusted using the built-in autocorrelated errors model (first-order autoregressive, AR(1)), accommodating serial correlation in consecutive annual rates.

The optimal number of joinpoints (0–5) was determined using a Monte-Carlo permutation test (4,499 permutations), with a significance level of 0.05 and Bonferroni correction for multiple testing. The software automatically selected the model that optimally balanced goodness-of-fit and parsimony. Segment-specific annual percent change (APC) and the average APC (AAPC) for the entire study period (1996–2022) were calculated with 95%CIs. The results of APC and AAPC analyses, together with raw annual case counts for each Joinpoint segment of total solid malignancies, lymphoma, CNS tumors, and SNS tumors in the nationwide referral cohort (1996–2022), are presented in Supplementary Table S1. Sensitivity analyses using aggregated strata were conducted to stabilize segments with low case counts. Model diagnostics, including permutation p-values and segment stability, are summarized in Table S2.

Age–Period–Cohort Analysis

Age–period–cohort effects on referral-based tumor occurrence were modeled using generalized linear models for count data with a log link and an offset for the log of the population at risk. Models were fitted in R (version 4.4.3) using glm() (base R) with family = quasipoisson(link = "log") to account for overdispersion and provide robust rate estimates. Poisson (glm(…, family = poisson())) and negative-binomial (MASS:: glm.nb()) models were inspected as sensitivity analyses.

Age, period, and cohort were treated as ordered factors using orthogonal polynomial contrasts (contr.poly), so. L,.Q,.C, and ^k terms represent linear, quadratic, cubic, and higher-order trends across ordered levels. Coefficients labeled Age_Group. L, Age_Group. Q, Period. L, Period. Q, Period. C, and Period^4–Period^8 therefore reflect trend effects across groups rather than exact category-specific rate ratios.

To address sparse cells in the age × period × cohort table, cohorts were collapsed into 2–3-year groups and sparse period categories were combined as necessary. Reference categories were set explicitly (Age = 0–4; Period = 1996–1998; Cohort = 1995). Sensitivity analyses were performed using sum-to-zero constraints (contr.sum) and broader grouping of sparse strata. Predictions and plots are based on the final quasi-Poisson APC model with collapsed strata and should be interpreted as smoothed age, period, and cohort effects, not exact cell-specific rates.

Robust standard errors, z-values, *P*-values, and 95%CI were calculated using lm test:: coeftest() with a sandwich estimator of variance. Results describing the directional trends of age, period, and cohort effects for lymphoma, CNS tumors, and SNS tumors in the nationwide referral cohort (1996–2022) are presented in Tables S3–S5. Model diagnostics, including dispersion parameters, residual deviance, and AIC/BIC statistics, are reported in Table S6. Additional details of the age–period–cohort analysis is provided in Supplementary Methods A.

All age–period–cohort estimates represent referral-based diagnosis patterns and may reflect changes in referral behavior, diagnostic practices, or hospital catchment in addition to underlying disease dynamics.

Incidence Rate Ratios (IRRs)

Temporal trends in referral-based tumor occurrence were assessed by calculating referral-based IRRs across consecutive 9-year calendar periods (1996–2004, 2005–2013, 2014–2022). The first period (1996–2004) and the 0–4 years age group were used as the dual reference category. To rigorously model these rates and address the inherent challenges of low case counts and data sparsity, particularly in the shorter periods, we first implemented data aggregation into the 9-year structure to increase the count stability in each stratum.

We employed a regression-based approach using Generalized Linear Models (GLMs). Specifically, tumor incidence was modeled as a function of age group, calendar period, and their interaction, incorporating the natural logarithm of the Person-Years At Risk (log (PYAR) as an offset term to directly estimate referral-based rates. Crucial change regarding the response variable and correction: The response variable used in the regression models was the raw integer case count (N), as the use of the Haldane–Anscombe 0.5 correction (N+0.5) in the response variable caused non-convergence errors due to the non-integer input violating the assumptions of the Negative Binomial and Poisson likelihood functions. However, the 0.5 correction was still applied to the raw counts for the calculation of descriptive rates.

We attempted to utilize Negative Binomial Regression (implemented via the glm.nb function in R's MASS package), which is robust to overdispersion common in count data. This model was successfully applied to lymphoma, though some instability in standard error estimation was noted. Due to persistent data sparsity and recurring convergence failures in the 9-year aggregated data, even with increased iteration limits, the models for CNS and SNS tumors were derived using Standard Poisson Regression (family = poisson). This mixed-modeling approach was statistically necessary to obtain stable and estimable rate ratios for all three tumor types.

Although different model families were employed, comparability across tumor types was maintained because all models estimated log-linear incidence rate ratios using identical covariate structures, offsets (log person-years), aggregation schemes, and reference categories. The resulting IRRs therefore represent internally consistent relative changes over time within each tumor type rather than direct cross-tumor risk comparisons. Differences in model family affect variance estimation but not the interpretation of the rate ratios themselves, which remain comparable as measures of temporal change in referral-based diagnosis rates.

Final IRRs and their 95% CIs for each age-period stratum were calculated by extracting the estimated marginal means from the fitted regression models (using the emmeans package) and dividing these estimates by the reference rate (0–4 years, 1996–2004). The resulting 95% CIs, derived directly from the regression models, are reported in Table S7.

Mann–Kendall Trend Test

The Mann–Kendall test was used to detect monotonic trends in tumor counts over the study period. This test complements model-based analyses but does not account for variations due to referral patterns or population changes; thus, conclusions were drawn primarily from APC and Joinpoint analyses rather than from Mann–Kendall results alone.

Population Denominators

For the primary analyses, national pediatric population counts stratified by sex and four age groups (< 1, 1–4, 5–9, and 10–14 years) were obtained from the Statistical Center of Iran (SCI) and United Nations data.[12] For

sensitivity analyses restricted to the Tehran Province, population denominators were derived from census and statistical yearbook data published by the Management and Planning Organization of Tehran (MPOT),[13] with established estimation methods applied to interpolate missing years (see Supplementary Methods B).

Population denominators were used solely for standardization purposes and do not imply that the resulting rates represent true population-level incidence.

Assessment of Potential Hospital-Level Drivers

To ensure that observed temporal trends reflected true changes rather than shifts in hospital capacity, referral patterns, or diagnostic capabilities, supplementary analyses were performed, including:

1. The annual proportion of solid tumor cases relative to total non-oncology pediatric elective surgeries (1996–2022);
2. The annual proportion of oncology caseloads relative to total non-oncology pediatric elective surgeries (1996–2022);
3. The distribution of referring provinces and the number of provinces represented for each year.

These analyses, presented in Tables S8 and S9 and Figure S1, support that the observed trends primarily reflect genuine temporal changes.

Statistical Significance

All tests were two-sided, and a P-value < 0.05 was considered statistically significant. Age-standardized incidence rates were calculated using the WHO standard population.[14] All analyses, figures, and tables are described in the main text, with full details, code, and diagnostics reported in the Supplementary Methods to ensure transparency and reproducibility.

Given the large number of stratified analyses (by tumor type, sex, age group, and calendar period), overall multiplicity across all subgroup comparisons was not addressed through global statistical correction beyond the Bonferroni procedure used for Joinpoint model selection. Instead, multiplicity was handled through cautious interpretation. Accordingly, subgroup-specific Joinpoint, Age–Period–Cohort, and Mann–Kendall results are considered exploratory and hypothesis-generating, and no definitive or confirmatory inference is drawn from secondary analyses.

Results

Demographics and Tumor Distribution

From 1996 to 2022, a total of 2,579 children with solid malignant tumors were diagnosed in our center. The majority were aged 1–4 years (45.1%), followed by 5–9 years (27.8%), 10–14 years (14.9%), and infants < 1 year (12.2%) (Figure 1A). Males comprised 55.4% of patien ts (M: F ratio 1.24), with a significantly higher proportion in the 5–9 age group ($P = 0.021$).

CNS and SNS tumors represented the largest tumor categories (40.8%), followed by lymphomas (16.7%), germ cell tumors (8.1%), hepatic tumors (5.3%), and bone tumors (2.6%) (Figure 1B). Lymphomas were significantly male-predominant (71% vs. 29%, $P < 0.001$), whereas germ cell tumors were female-predominant (63.2% vs. 36.8%, $P < 0.001$) (Figure 1C). Age distributions differed significantly across most tumor types: soft tissue sarcomas, SNS, hepatic, renal, and germ cell tumors were concentrated in younger ages, whereas bone tumors and lymphomas peaked in older children (Figure 1D).

Figure 1E shows annual frequencies of newly diagnosed total solid tumors in our center (1996–2022), displayed in a heatmap format with color intensity reflecting case volume (from 37 cases in 2001 to 189 cases in 2018).

Overall Temporal Trends

Temporal trends in pediatric solid malignancies were initially evaluated using Joinpoint regression applied to annual referral-based case counts standardized to the national pediatric population for temporal comparison purposes, allowing assessment of changes in population-standardized referral-based rates over time. This analysis identified three distinct temporal phases in the population-standardized rates (Figure 2A): a non-significant early decline from 1996–2004 (APC = –1.93%, 95% CI: –20.69 to 4.90; P = 0.575), followed by a marked increase from 2004–2014 (APC = 13.82%, 95% CI: 10.04 to 35.35; $P = 0.004$), and a subsequent stabilization from 2014–2022 (APC = 1.03%, 95% CI: –4.88 to 4.47; $P = 0.316$). Given the short duration and wide confidence intervals of some segments, interpretation focused primarily on the overall AAPC, which demonstrated a statistically significant increasing trend across the full study period (AAPC = 4.81%, 95% CI: 3.35–6.42; $P < 0.001$). Accordingly, segment-specific APC estimates are presented for completeness but should be considered exploratory and not interpreted as stable or definitive temporal effects. This finding was independently supported by the Mann–Kendall trend test, which showed a significant monotonic upward trend over time ($\tau = 0.692$, $P < 0.001$).

Because these analyses are based on referral counts from a single tertiary center, observed changes in referral-based population-standardized rates may reflect not only underlying disease dynamics but also temporal changes in referral patterns, diagnostic availability, hospital capacity, or catchment area. Accordingly, all trend estimates are interpreted as indicators of referral-based temporal dynamics rather than direct measures of national incidence.

Crude rates showed a similar trend, including a short, statistically unstable spike from 2009–2011, with an overall AAPC of 6.03% (95% CI: 4.59–7.66; $P < 0.001$) (Figure 2B, Table S1).

Temporal Trends by Tumor Type (Overall Referral-Based Rates)

Analyses of overall referral-based population-standardized rates demonstrated statistically significant increasing

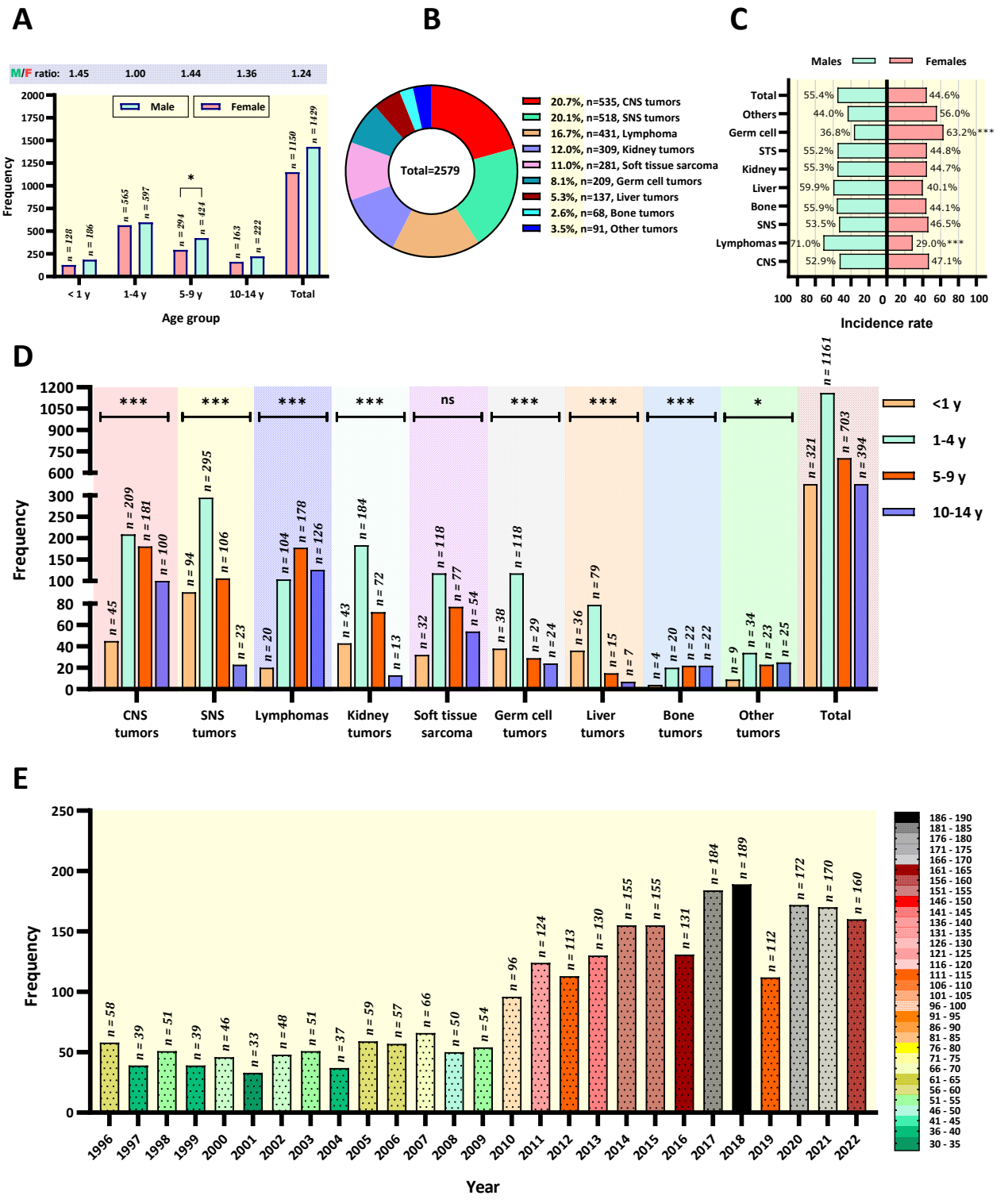

Figure 1. Demographic and Tumor Diagnosis Characteristics of the Studied Population. This figure provides an overview of the demographic distribution within the studied population and key characteristics of tumor diagnoses. (A) Distribution of Sexes Across Age Groups: This panel displays the distribution of male and female individuals within different age categories. (B) Relative Frequency of Tumor Types: This pie chart illustrates the proportional representation of various tumor types observed in the study. (C) Distribution of Tumors by Sex: This butterfly graph depicts the distribution of all tumors across male and female individuals. (D) Distribution of Tumors by Age Group: This column graph presents the distribution of all tumors across different age groups. (E) Temporal Trend in Total Solid Tumor Diagnoses: This panel shows the annual number of newly diagnosed total solid tumors over time in the studied population. The columns are color-coded in a heatmap-like manner, ranging from light green (lowest frequency) to dark black (highest frequency) to visually represent the yearly incidence frequency. Statistical significance is denoted by asterisks: *P < 0.05, **P < 0.01, and ***P < 0.001. The absence of an asterisk indicates no statistically significant difference. All frequencies shown represent referral-based case counts rather than population-level incidence [Abbreviation: CNS, Central Nervous System; SNS, Sympathetic Nervous System; STS, Soft Tissue Sarcoma; y, years of age].

temporal trends for all three major pediatric tumor groups over the 1996–2022 study period (Figure 3A–F). Based on crude referral-based rates, Joinpoint regression identified sustained upward trends for lymphomas, CNS tumors, and SNS tumors. Specifically, the lymphoma crude rates increased with an average annual percent change (APC) of 3.52% (95% CI: 2.35–5.00; $P<0.001$), the CNS tumor crude rates rose more steeply (APC = 7.56%; 95% CI: 5.88–10.47; $P<0.001$), and the SNS tumors exhibited the largest increase (APC = 8.49%; 95% CI: 6.69–11.80; $P<0.001$) over the study period (Figure 3A–C).

When summarized using average annual percent change (AAPC), crude referral-based trends yielded identical estimates, reflecting a single dominant long-term trend segment for each tumor group (Table S1). This concordance supports the robustness of the observed long-term increases and reduces reliance on short-term segment-specific fluctuations.

When age adjustment was applied using population denominators as analytical references, similar long-term patterns were observed (Figure 3D–F). Age-adjusted referral-based rates increased steadily for lymphomas (APC = 3.55%; 95% CI: 2.31–4.79; $P<0.001$), CNS tumors (APC = 6.35%; 95% CI: 3.56–9.36; $P<0.001$), and SNS tumors (APC = 8.94%; 95% CI: 6.37–11.60; $P<0.001$). For all tumor types, Joinpoint models identified a single dominant long-term trend without additional joinpoints, indicating consistent increases in referral-based diagnosis rates across the study period.

Importantly, these crude and age-adjusted estimates reflect population-standardized referral patterns within a single tertiary pediatric oncology center rather than true population-based incidence. The observed increases may therefore reflect evolving referral practices, diagnostic capacity, disease awareness, and changes in hospital catchment, in addition to any underlying temporal changes in disease occurrence.

Stratified analyses by age group and sex, which showed greater heterogeneity and short-term fluctuations, are presented in the Supplementary Material (Figures S2–S4) and should be interpreted as exploratory.

Age–Period–Cohort Analysis

Age–Period–Cohort modeling was applied to describe smoothed temporal components underlying referral-based pediatric tumor diagnosis patterns while explicitly acknowledging the inherent non-identifiability of age, period, and cohort effects. Accordingly, Age–Period–Cohort outputs were interpreted as descriptive trend components rather than directly estimable age-, period-, or cohort-specific incidence or risk. In the main analysis, interpretation focused primarily on calendar

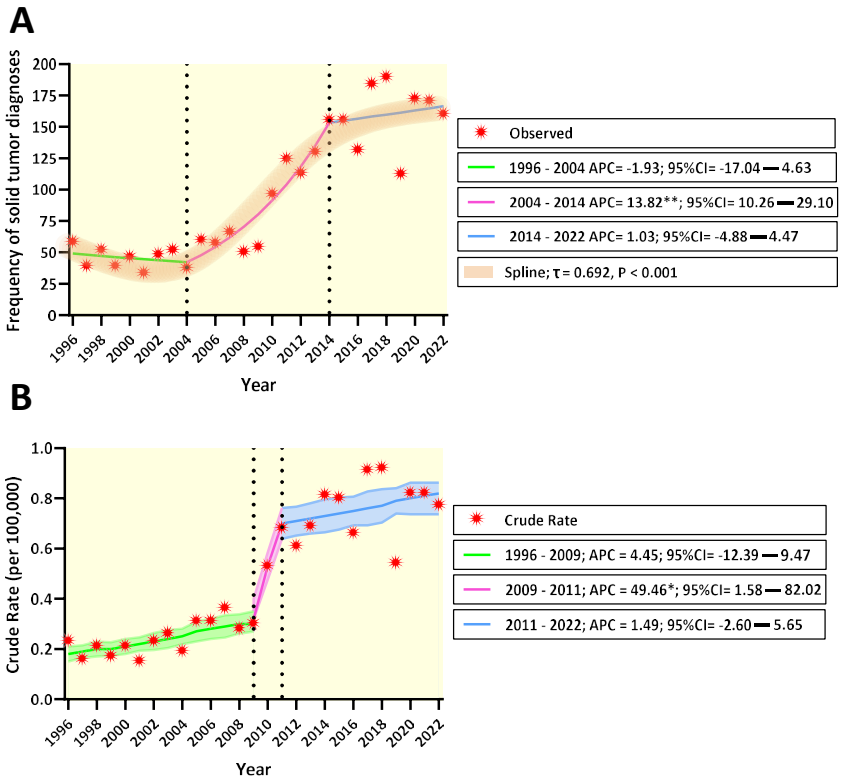

Figure 2. Temporal Trends in Total Solid Tumor Diagnoses and Annual Percent Change (APC). (**A**) Frequency of Total Solid Tumors and Joinpoint Analysis: Raw counts of total solid tumors over the study period are shown, with Joinpoint analysis results overlaid. Smoothed trend lines for the counts are depicted as shaded areas around the APC curve. (**B**) Observed Crude Referral-Based Rates and Joinpoint Analysis: Crude rates are represented by symbols, with APC curves shown as solid lines. Shaded areas indicate standard errors around the APC curve. Joinpoints are marked by vertical dashed lines on the x-axis. APC curve colors indicate different trend segments: green for the segment before the first Joinpoint, pink after the first, and light blue after the second. Statistical Annotations: Mann–Kendall test statistics and APC values are indicated. Statistical significance is denoted by asterisks: *$P<0.05$, **$P<0.01$, ***$P<0.001$; absence of an asterisk indicates no statistically significant trend. Crude rates are calculated using population denominators as analytical references and reflect referral-based temporal patterns rather than population incidence [Abbreviations: APC, annual percent change; CI, confidence interval; τ, Mann-Kendall trend test].

period effects, which emerged as the most stable and interpretable components across tumor types. Detailed age- and cohort-related model outputs are presented in the Supplementary Material (Tables S3–S5; Figure S5).

Across tumor groups, calendar period components suggested an overall upward temporal pattern in referral-based diagnosis rates, most clearly for CNS tumors and more directionally for SNS tumors (Figures 4B and 4C). For CNS tumors, predicted period-specific diagnosis rates exhibited an overall upward trend from the mid-2000s onward, with non-monotonic fluctuations between adjacent calendar periods. This pattern was supported by statistically significant linear and higher-order orthogonal polynomial period terms in the Age–Period–Cohort model, which characterize the overall temporal shape rather than directly estimable period-specific effects (Table S4).

For SNS tumors, Age–Period–Cohort modeling suggested a directional positive calendar period component in referral-based diagnosis patterns (Figure 4C). This was primarily reflected by statistically significant linear and selected higher-order orthogonal polynomial period terms (Table S5). However, period-specific estimates for SNS tumors were highly variable and accompanied by wide confidence intervals, reflecting substantial data sparsity and the necessity of aggregating calendar periods for model stability. Accordingly, the SNS period effect should be interpreted as a smoothed, descriptive temporal component indicating overall directional change rather than a stable or precisely estimated period-specific pattern.

Lymphomas demonstrated more heterogeneous period-related patterns. While individual period-specific estimates varied, the Age–Period–Cohort model identified a significant positive linear period component, indicating an overall increase in referral-based diagnosis rates over time after adjustment for age and cohort components (Figure 4A; Table S3). As with CNS and SNS tumors, higher-order period terms reflected complex temporal curvature rather than discrete, directly interpretable period effects.

Across all tumor types, the age- and cohort-related components displayed greater variability and sensitivity to sparse strata. Cohort estimates, in particular, were unstable and frequently accompanied by wide confidence intervals, underscoring the limitations of cohort interpretation in single-center, referral-based Age–Period–Cohort analyses. These components are therefore presented in the Supplementary Material (Table S3-S5; Figure S5) and interpreted strictly as smoothed descriptive patterns, not

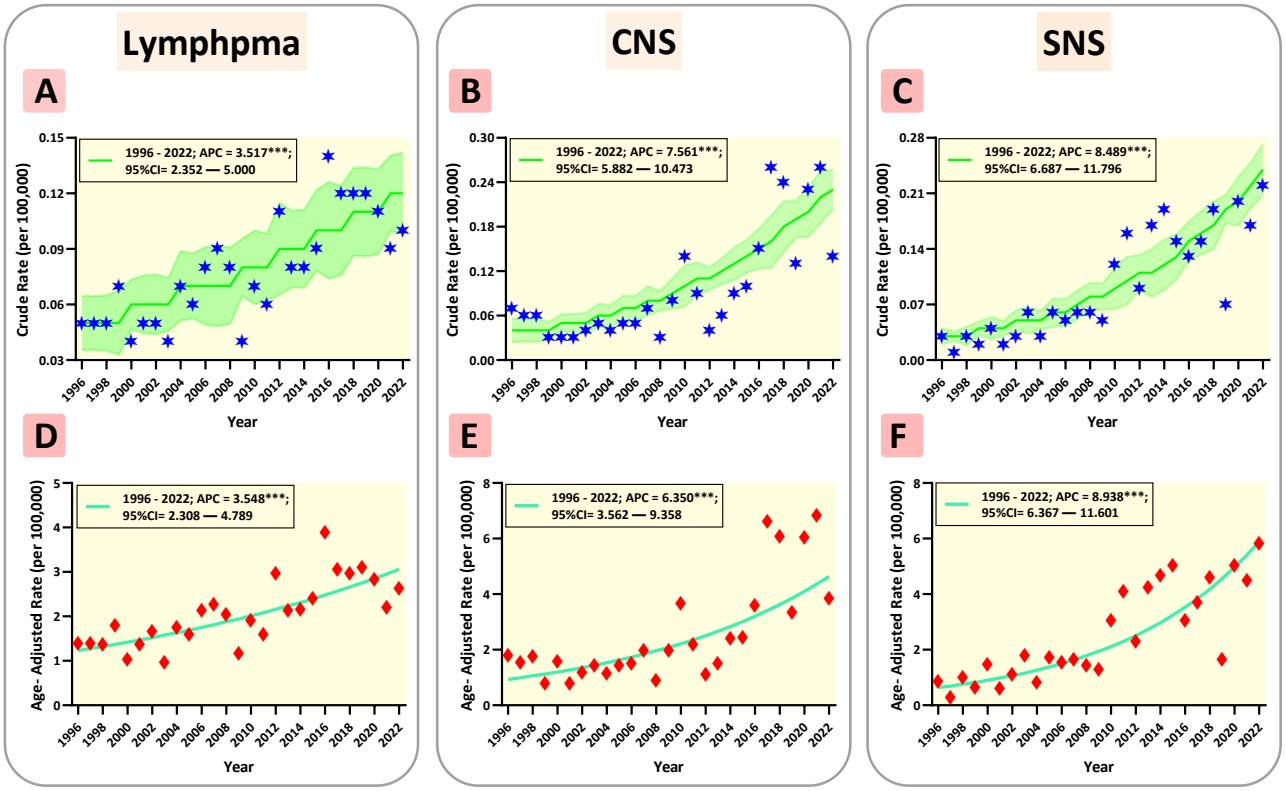

Figure 3. Annual Percent Change (APC) of Lymphomas, Central Nervous System (CNS) Tumors, and Sympathetic Nervous System (SNS) Tumors (total cases). This figure illustrates the referral-based rate changes of common pediatric tumors. (**A**) APC and identified joinpoints (points where the trend significantly changes) for Lymphomas based on crude incidence rates. (**B**) APC and identified joinpoints for CNS based on crude incidence rates. (**C**) APC and identified joinpoints for SNS based on crude incidence rates. (**D**) APC and identified joinpoints for age-adjusted incidence rates for Lymphomas. (**E**) APC and identified joinpoints for age-adjusted incidence rates for CNS. (**F**) APC and identified joinpoints for age-adjusted incidence rates for SNS. Observed crude rates are represented by symbols. APC curves are shown as solid lines, with their standard errors indicated by the shaded areas above and below the main curve. Statistical Annotations: APC values are provided on each panel in boxes. Statistical significance is denoted by asterisks: *P<0.05, **P<0.01, and ***P<0.001. The absence of an asterisk indicates no statistically significant difference. All rate estimates are referral-based and intended for relative temporal comparisons rather than estimation of true population incidence [Abbreviation: APC, Annual Percent Change; CI, confidence interval; CNS, Central Nervous System; SNS, Sympathetic Nervous System].

as evidence of cohort-specific disease risk differences.

Overall, Age–Period–Cohort modeling indicated that calendar period–related influences were the dominant contributors to long-term changes in referral-based pediatric tumor diagnosis patterns in this center. Age effects were tumor-specific, while cohort effects were variable and less stable. These findings highlight the importance of cautious interpretation of Age–Period–Cohort outputs and suggest that temporal changes in diagnostic practices, referral pathways, and healthcare system factors likely played a central role in shaping observed long-term trends.

ASIRs and IRRs

Over the 27-year study period (1996–2022), referral-based ASIRs for lymphomas, CNS tumors, and SNS tumors exhibited gradual upward temporal trends (Figure 5A). These patterns were broadly consistent across tumor types, although the magnitude and stability of increases varied.

To enhance statistical stability, IRRs were calculated using three aggregated 9-year periods (1996–2004, 2005–2013, and 2014–2022) and should be interpreted as relative temporal changes in referral-based diagnosis rates rather than as direct measures of disease risk. The resulting IRRs, presented by age group and tumor type, are shown in Figures 5B–D and Table S7.

Within each tumor group, analyses consistently indicated higher referral-based diagnosis rates in the most recent calendar period (2014–2022), although the magnitude and stability of these increases varied by age and tumor type. For lymphomas, referral-based rates remained relatively stable across earlier periods but showed a generalized increase across all age groups in the final period, with the highest relative elevation observed in the 5–9-year age group (IRR = 2.78; 95% CI: 2.24–3.45). CNS tumors demonstrated progressive increases over time, particularly in the 0–4- and 5–9-year age groups, while patterns in older children were more variable. SNS tumors exhibited the largest relative increases, driven predominantly by the youngest age group, whereas estimates for older age groups showed marked variability.

Several IRR estimates (most notably among older age groups and in earlier calendar periods) were derived from very small stratum case counts and should therefore be interpreted as statistically unstable and exploratory. In particular, SNS estimates for the 5–9-year age group in the 1996–2004 period and the 10–14-year age group in the 1996–2004 and 2005–2013 periods (corresponding to data points enclosed by dashed circles in Figure 5D) were based on extremely sparse data (e.g. $N \leq 10$ per stratum; Table S7) and should be therefore interpreted cautiously due to substantial statistical uncertainty, as reflected by wide confidence intervals.

As detailed in the Methods section, all IRRs represent relative temporal changes in referral-based diagnosis rates within tumor types and should not be interpreted as precise risk estimates or as directly comparable measures across tumor groups.

Shifts in Tumor Proportions

The relative contributions of tumor types changed over time (Figure 6). Lymphomas initially comprised a large share but declined in the mid-2000s before recovering slightly. CNS tumors increased their proportional representation, particularly after 2014, while SNS tumors rose steadily, reaching 28.1% of all cases in 2022 (Figure 6A). Within-group analyses demonstrated significant year-to-year distributional changes, especially after 2011 ($P < 0.001$ in several years), largely due to rising contributions of CNS and SNS tumors (Figure 6B).

These proportional shifts reflect changing referral-based case composition over time and should not be interpreted as definitive changes in population-level tumor incidence.

Discussion

This retrospective study examined the referral-based epidemiology and temporal diagnosis patterns of solid malignant tumors in 2,579 Iranian children diagnosed at Mofid Pediatric Hospital between 1996 and 2022. As

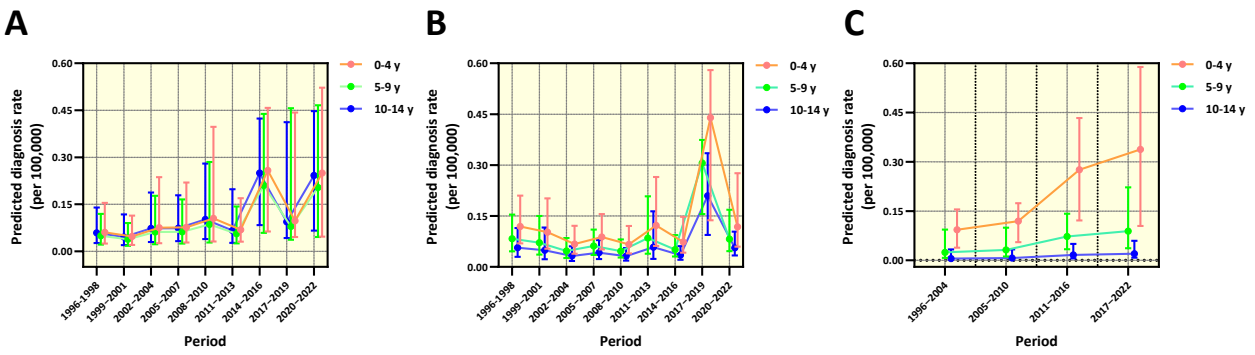

Figure 4. Period-specific predicted referral-based diagnosis rates for pediatric solid tumors (1996–2022). (**A**) Period-specific rates for Lymphomas. (**B**) Period-specific rates for Central Nervous System (CNS) Tumors. (**C**) Period-specific rates for Sympathetic Nervous System (SNS) Tumors. All rates are expressed per 100,000 population. Error bars represent 95% confidence intervals derived from the quasi-Poisson age–period–cohort models. For SNS tumors, fewer and wider calendar periods (four instead of nine) are shown because sparse original period categories were collapsed into four estimable groups and encoded using three orthogonal polynomial contrasts (Period. L, Period. Q, and Period.C). All estimates are model-based predictions and should be interpreted as smoothed period effects rather than exact cell-specific rates. For clarity in visualization, some symbols were slightly offset along the x-axis [Abbreviation: y, years].

a major national referral center, Mofid Pediatric Hospital receives cases from across the nation, offering a unique opportunity to analyze a large and diverse cohort. However, data from a single tertiary referral institution, while comprehensive for this referral population, do not represent true national incidence and are inherently influenced by referral dynamics. Our primary objective was not to estimate countrywide incidence rates, but rather to investigate long-term temporal trends in tumor distribution and referral-based population-standardized occurrence patterns over a 27-year period, thereby providing insight into evolving patterns of pediatric solid malignancies in Iran.

Key Findings and Global Context

The largest cohort comprised children aged 1–4 years, with CNS and SNS tumors being most frequent, together accounting for 40.8% of cases. Lymphomas showed a significant male predominance (71%), while germ cell tumors were more common in females (63.2%).

Our findings confirm global patterns: most pediatric solid tumors occur in early childhood, especially embryonal tumors such as neuroblastoma, Wilms tumor, and hepatoblastoma.[15-17] Bone tumors and lymphomas peak later, consistent with their biological links to skeletal growth and immune maturation.[18,19] Gender disparities also matched prior data, with male predominance in lymphomas and female predominance in germ cell tumors.[20-23]

Overall Temporal Trends

Joinpoint regression analysis demonstrated a significant overall rise in referral-based diagnosis patterns, with AAPCs of 4.81% for referral-based population-standardized rates and 6.03% for crude referral-based rates. When examined by major tumor group, lymphomas, CNS tumors, and SNS tumors all demonstrated sustained increases in overall referral-based population-standardized rates across the study period. These long-term increases were robust to analytic approach, with concordant findings across crude and age-adjusted analyses and no evidence of multiple unstable joinpoints

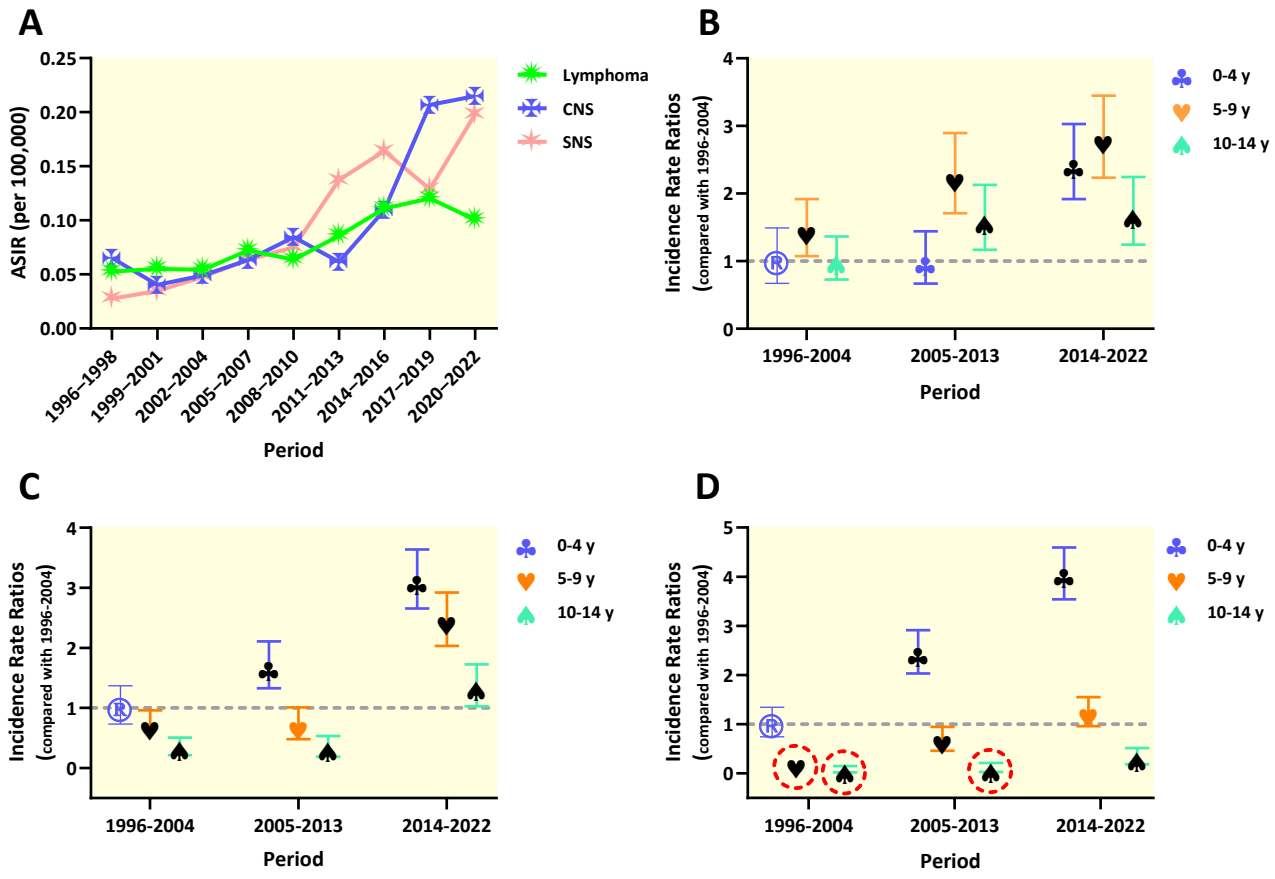

Figure 5. Temporal Trends in Pediatric Solid Tumors: Referral-Based Age-Standardized Rates and Incidence Rate Ratios by Tumor Type and Age Group. (**A**) Referral-based age-standardized incidence rates (ASIRs) for Lymphomas, CNS tumors, and SNS tumors over the 1996–2022 period, standardized to the WHO 2000–2025 pediatric population. (**B–D**) Model-based incidence rate ratios (IRRs) comparing three 9-year calendar periods (2005–2013 and 2014–2022) with the reference period (1996–2004) within each age group for (**B**) Lymphomas, (**C**) CNS tumors, and (**D**) SNS tumors. IRRs were estimated using tumor-specific generalized linear models with a log(person-years) offset and represent relative changes in referral-based diagnosis rates, not absolute population risks. A horizontal dashed line denotes IRR = 1. The reference groups are indicated by ® Black symbols denote estimates that differ statistically from the reference category, with values above the IRR = 1 line indicating relative elevation and values below the line indicating relative reduction. Data points encircled with dashed circles are based on very small stratum-specific case counts (typically N ≤ 10) and therefore represent statistically unstable estimates; these are displayed for completeness and should be interpreted as exploratory. Error bars denote 95% confidence intervals. Detailed numerical values and raw counts are provided in Supplementary Table 7 [Abbreviation: ASIR, Age-Standardized Incidence Rate; CNS, Central Nervous System; SNS, Sympathetic Nervous System; y, years of age].

in tumor-specific models. This consistency supports the presence of broad, monotonic temporal shifts in referral-based diagnosis patterns rather than isolated short-term anomalies.

The upward trajectory is directionally consistent with global reports of increasing childhood cancer incidence, although direct comparisons should be interpreted cautiously given the referral-based design of the present study.[24,25] National registry data from Iran similarly indicate a growing burden: Jorjani et al. (2024)[9] reported rising pediatric cancer diagnoses between 2014 and 2018, and Shabani et al. (2019)[10] documented increasing cancer incidence and mortality from 1990 to 2016. Improved diagnostics, better healthcare access, and awareness likely contribute,[4,26] though environmental factors, particularly urban air pollution, may play a role.[27]

Accordingly, while similarities with population-based registry findings are notable, the increases observed in this study should be interpreted primarily as temporal changes in referral-based diagnosis patterns rather than direct estimates of national incidence. Importantly, supplementary internal benchmark analyses (Figure S1; Tables S8–S9) demonstrated temporal stability in overall hospital capacity and referral catchment, while oncology-related activity increased relative to this stable denominator. This pattern suggests that abrupt shifts in capacity or preferential referral are unlikely to be the sole explanation and supports interpretation of the findings in terms of robust long-term temporal dynamics in pediatric oncology case burden, within the acknowledged limitations of a single-center referral-based design.

CNS and SNS tumors exhibited steeper increases than lymphomas, a pattern consistent with prior reports from both population-based registries and referral-center studies.[28,29] While improved neuroimaging availability and heightened diagnostic sensitivity likely contributed to rising CNS tumor detection,[30] the persistence of upward trends in age-adjusted referral-based rates suggests that

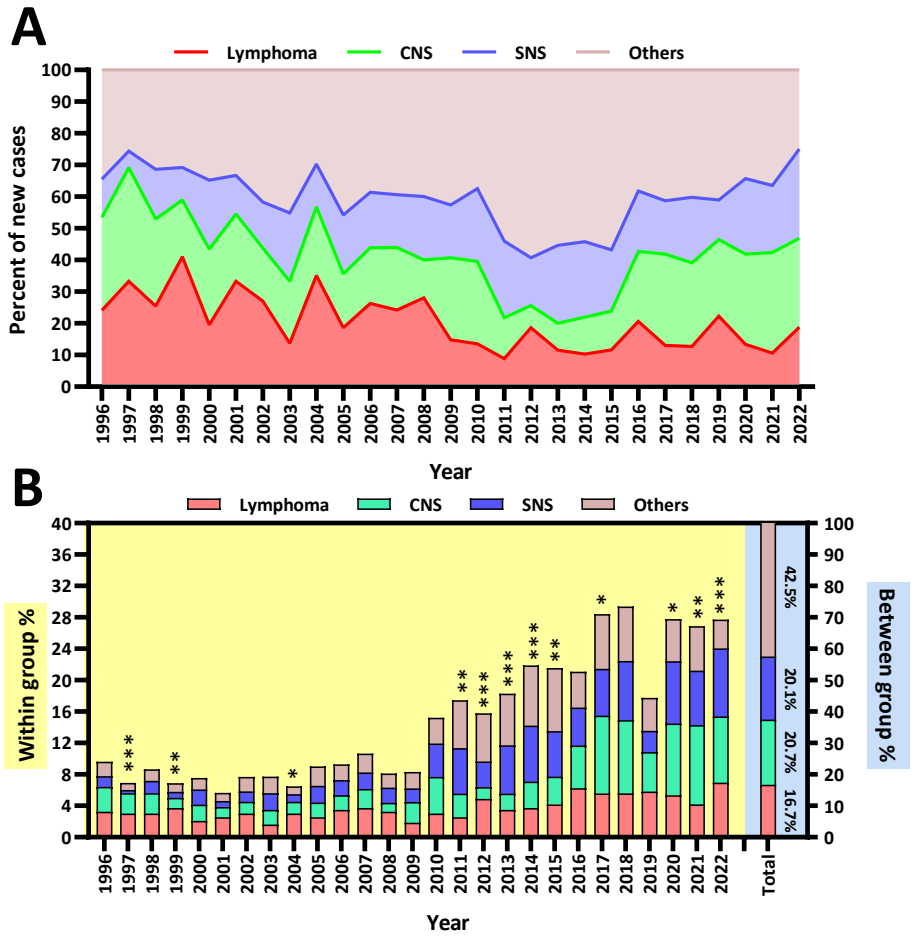

Figure 6. Temporal Changes in the Distribution of Pediatric Solid Malignant Tumors in a Major Iranian Pediatric Referral Center (1996–2022). (**A**) Between-Group Proportional Representation: The cumulative line plot with shaded areas shows the annual proportional contribution of Lymphomas, Central Nervous System (CNS) tumors, Sympathetic Nervous System (SNS) tumors, and "other" tumors to the total solid tumor caseload. Each point represents the percentage of a specific tumor group relative to all solid tumor cases diagnosed in that year. (**B**) Within-Group Temporal Distribution: This stacked column chart displays the annual percentage of each tumor type relative to its total cases across the entire study period (1996-2022). The Total column, at the far right of Figure 7B, encapsulates the overall proportional distribution of the studied malignancies across the entire study cohort (1996-2022). This column visually represents the aggregated 'between-group distribution' for the full period, demonstrating the relative contribution of each tumor type to the total caseload. The specific percentage for each malignancy is clearly indicated adjacent to its corresponding stacked segment. Stars indicate the statistical significance of the annual distribution alterations as determined by Chi-squared or Fisher's exact test (calculated in a 4x2 table comparing within-group percentages for each tumor type against the complement for that year): *P<0.05, **P<0.01, and ***P<0.001. Proportions are calculated within the referral cohort and do not represent national population distributions. [Abbreviation: CNS, Central Nervous System; SNS, Sympathetic Nervous System].

diagnostic factors alone may not fully explain the observed patterns.[31] Similarly, the pronounced increases observed for SNS tumors, predominantly neuroblastomas and most evident in early childhood, align with international observations[28,32] but must be interpreted cautiously in light of referral-based ascertainment.

Age–Period–Cohort Effects

Age–Period–Cohort modeling was used as a descriptive framework to decompose smoothed temporal components underlying referral-based diagnosis patterns, rather than to infer etiologic risk. Given the inherent non-identifiability of Age–Period–Cohort models and the referral-based nature of the data, interpretation appropriately focused on calendar period effects, which emerged as the most stable and consistent component across tumor types.

CNS and SNS tumors demonstrated strong and sustained positive period effects beginning in the mid-2000s, indicating that temporal factors acting uniformly across age groups (such as improvements in diagnostic infrastructure, referral networks, and healthcare access) were dominant contributors to the observed increases in referral-based diagnosis rates. Lymphomas showed more heterogeneous period patterns, although an overall positive linear period trend remained evident after adjustment for age and cohort components.

Age and cohort effects displayed greater variability and sensitivity to sparse strata, particularly for SNS tumors. These components are therefore best interpreted as smoothed trend descriptors rather than cohort-specific risk estimates. Apparent cohort-related fluctuations may reflect residual identifiability constraints, sparse data, or shifting referral dynamics rather than true generational differences in disease occurrence. Overall, the Age–Period–Cohort findings reinforce the central role of time-related system-level influences in shaping long-term referral-based diagnosis patterns at this center.[33]

ASIRs, IRRs, and Tumor Distribution

Referral-based ASIRs and IRRs provided complementary summaries of long-term temporal change. Gradual increases in referral-based ASIRs across all three tumor groups were consistent with Joinpoint and Age–Period–Cohort findings, reinforcing the presence of sustained upward trends over nearly three decades. To enhance statistical stability, IRRs were estimated using aggregated 9-year periods and should be interpreted as relative temporal changes in referral-based diagnosis rates, not as measures of absolute or population-level cancer risk.

Across tumor types, the most notable pattern was a pronounced increase in referral-based rates during the most recent period (2014–2022), particularly for CNS and SNS tumors and most prominently in younger children, while increases for lymphomas were more modest.[34,35] These patterns likely reflect a convergence of improved diagnostic access, earlier detection, evolving referral behavior, and possibly changes in underlying disease burden.[36,37] However, several IRR estimates (especially those derived from older age groups and earlier periods) were based on very small case counts and are therefore statistically unstable.

Notably, the composition of tumor types shifted over time. Lymphomas initially represented the largest proportion of cases but declined in the mid-2000s before a modest recovery, whereas CNS tumors increased their relative representation, particularly after 2014. SNS tumors rose steadily throughout the study period, reaching 28.1% of all cases by 2022. These evolving proportions, alongside the ASIR and IRR trends, underscore the growing contribution of CNS and SNS tumors to the overall pediatric oncology caseload.

Two key points should be emphasized. First, although IRRs and ASIRs are derived from referral counts standardized to external population denominators, they reflect relative temporal changes in referral-based diagnosis rates rather than direct measures of population-level risk. Notably, the center's referral catchment has remained broadly stable over time and includes a majority of cases from outside Tehran (57.6–67.0% annually; Table S8), resembling national referral patterns and providing a reasonably representative sample. Nevertheless, these statistics should be still interpreted as indicators of relative temporal trends rather than definitive population-level incidence. Second, differences in model specification (Poisson vs. negative binomial) across tumor types reflect underlying distributional properties of the data rather than substantive differences in interpretation. Within each tumor group, IRRs remain valid indicators of relative temporal trends, but cross-tumor comparisons should be interpreted qualitatively rather than quantitatively. Overall, the ASIR and IRR analyses consistently indicate that more recent calendar periods were associated with substantially higher referral-based pediatric tumor diagnoses in this center.

Limitations

This study has some limitations. First, as a single-center referral-based cohort, the findings do not represent true population-level incidence and may be influenced by referral patterns, case-mix differences, and access to specialized care.[38] Although Mofid Pediatric Hospital functions as a major national referral center, referral bias cannot be fully excluded. To address this, we performed multiple sensitivity and validation analyses, including an assessment of the geographic stability and breadth of the referral catchment over time and a sensitivity analysis restricted to the Tehran Province using local population denominators. These analyses demonstrated a consistently broad national referral scope and yielded temporal trends that were directionally concordant with the primary analyses. Nevertheless, uncertainty regarding the true population at risk remains an inherent limitation of referral-based studies. Even with stable geographic referral coverage, changes in referral thresholds, diagnostic intensity, and access to specialized pediatric

oncology services over time may have contributed to the observed trends.

Second, small case numbers for rare tumor subtypes limited statistical power in some stratified analyses and necessitated aggregation of age, period, or cohort categories in Joinpoint and Age–Period–Cohort models. As a result, short-term fluctuations and extreme segment-specific estimates should be interpreted cautiously, with greater emphasis placed on overall average annual percent changes and long-term trends. Additionally, the numerous subgroup analyses (by age, sex, and tumor type) raise the potential for inflated Type I error due to multiple testing; thus, significant findings in subgroups should be viewed as hypothesis-generating and requiring confirmation in larger datasets.

Third, Age–Period–Cohort analyses are subject to the well-known identifiability problem arising from the linear dependency between age, period, and cohort. Although we applied quasi-Poisson generalized linear models, orthogonal polynomial contrasts, sensitivity analyses with alternative parameterizations, and extensive diagnostic checks, residual confounding and model dependence on analytic choices cannot be entirely ruled out.

Fourth, the retrospective nature of the study introduces the potential for incomplete documentation, changes in diagnostic practices, evolving imaging availability, and improvements in pathological classification over time. These factors may have contributed to increased detection, particularly for CNS and SNS tumors, and may partially explain observed temporal increases. Although supplementary analyses suggested that changes in hospital capacity or elective surgical volume were unlikely to be the primary drivers of the observed trends, detection bias remains a plausible contributing factor.

Finally, the absence of survival data, treatment information, and etiological exposures (e.g. environmental, genetic, or perinatal factors) limits causal interpretation and precludes assessment of outcome trends alongside diagnostic patterns.

Conclusion

Over nearly three decades, this comprehensive single-center analysis from a major Iranian pediatric referral hospital demonstrates substantial and sustained increases in referral-based diagnoses of pediatric solid malignancies, particularly CNS and sympathetic nervous system tumors, across age groups and sexes. In contrast, lymphomas exhibited more heterogeneous temporal patterns, with weaker age effects and evidence of variability across birth cohorts.

Age–period–cohort modeling suggested that calendar period effects were the dominant contributors to observed temporal changes, suggesting that factors operating broadly over time (such as evolving diagnostic practices, environmental exposures, or health system–level changes) may play an important role. Although referral-based design limits inference regarding true population incidence, extensive sensitivity analyses, catchment stability assessments, and internal benchmarks support the robustness of the observed temporal patterns.

These findings highlight the growing clinical burden of pediatric solid malignancies presenting to major referral centers in Iran and underscore the need for strengthened population-based cancer registration, continued monitoring of temporal trends, and future studies integrating environmental, genetic, and health system data to better elucidate the drivers underlying these long-term changes.

Authors' Contribution

Conceptualization: Maryam Kazemi Aghdam, Gholamreza Ebrahimisaraj.
Data Curation: Maryam Kazemi Aghdam, Yalda Nilipour, Seiedehparnian Taghvaei, Gholamreza Ebrahimisaraj, Mehdi Sarafi.
Formal Analysis: Maryam Kazemi Aghdam, Bibi Shahin Shamsian, Samin Alavi, Nader Momtazmanesh, Peyman Eshghi, Gholamreza Ebrahimisaraj.
Funding Acquisition: No Fund Was Acquired.
Investigation: Maryam Kazemi Aghdam, Yalda Nilipour, Seiedehparnian Taghvaei, Bibi Shahin Shamsian, Samin Alavi, Nader Momtazmanesh, Peyman Eshghi, Gholamreza Ebrahimisaraj, Mehdi Sarafi, Leili Mohajerzadeh, Javad Ghoroubi, Mohsen Rouzrokh, Ahmad Khaleghnejad Tabari.
Methodology: Nader Momtazmanesh, Peyman Eshghi, Gholamreza Ebrahimisaraj, Mehdi Sarafi, Leili Mohajerzadeh, Javad Ghoroubi.
Project Administration: Maryam Kazemi Aghdam, Yalda Nilipour, Seiedehparnian Taghvaei, Bibi Shahin Shamsian, Samin Alavi, Nader Momtazmanesh, Peyman Eshghi, Gholamreza Ebrahimisaraj, Mehdi Sarafi, Leili Mohajerzadeh, Javad Ghoroubi, Mohsen Rouzrokh, Ahmad Khaleghnejad Tabari.
Resources: Maryam Kazemi Aghdam, Gholamreza Ebrahimisaraj, Mehdi Sarafi.
Software: Seiedehparnian Taghvaei, Bibi Shahin Shamsian, Gholamreza Ebrahimisaraj.
Supervision: Gholamreza Ebrahimisaraj.
Validation: Maryam Kazemi Aghdam, Yalda Nilipour, Mohsen Rouzrokh, Ahmad Khaleghnejad Tabari.
Visualization: Maryam Kazemi Aghdam, Gholamreza Ebrahimisaraj, Mehdi Sarafi.
Writing–Original Draft: Gholamreza Ebrahimisaraj, Mehdi Sarafi.
Writing–Review & Editing: Leili Mohajerzadeh, Javad Ghoroubi, Mohsen Rouzrokh, Ahmad Khaleghnejad Tabari.

Competing Interests

The authors declare no conflict of interest regarding this study and its publication.

Data Availability Statement

The data that support the findings of this study are available from the corresponding author upon reasonable request.

Ethical Approval

Approval for the research design was obtained from the Institutional Review Board and the Ethics Committee affiliated with Mofid Children's Hospital, following a thorough evaluation process. As the study was conducted retrospectively and relied solely on de-identified patient records, obtaining informed consent from individual participants was deemed unnecessary and formally exempted. To uphold patient privacy, all personal identifiers were removed from the data before any analysis, thereby safeguarding confidentiality throughout the research process.

Funding

This research did not receive any specific grant from funding

agencies in the public, commercial, or not-for-profit sectors.

Supplementary Files

Supplementary file 1 contains Table S1-S9 and Figures S1-S5.
Supplementary file 2. R Code for Reproducible Age–Period–Cohort, Incidence Rate Ratio, and Trend Analyses.

References

1. Huang J, Chan SC, Ngai CH, Lok V, Zhang L, Lucero-Prisno DE 3rd, et al. Global incidence, mortality and temporal trends of cancer in children: a joinpoint regression analysis. Cancer Med 2023;12(2):1903-11. doi:10.1002/cam4.5009
2. Smith L, Stiller CA, Aitken JF, Hjalgrim LL, Johannesen T, Lahteenmaki P, et al. International variation in childhood cancer mortality rates from 2001 to 2015: comparison of trends in the International Cancer Benchmarking Partnership countries. Int J Cancer 2022;150(1):28-37. doi:10.1002/ijc.33774
3. Filho AM, Laversanne M, Ferlay J, Colombet M, Piñeros M, Znaor A, et al. The GLOBOCAN 2022 cancer estimates: data sources, methods, and a snapshot of the cancer burden worldwide. Int J Cancer 2025;156(7):1336-46. doi:10.1002/ijc.35278
4. Sung H, Ferlay J, Siegel RL, Laversanne M, Soerjomataram I, Jemal A, et al. Global cancer statistics 2020: GLOBOCAN estimates of incidence and mortality worldwide for 36 cancers in 185 countries. CA Cancer J Clin 2021;71(3):209-49. doi:10.3322/caac.21660
5. Ilbawi A, Ortiz R, Fidarova E. CureAll Framework: WHO Global Initiative for Childhood Cancer: Increasing Access, Advancing Quality, Saving Lives. Geneva: World Health Organization; 2021. Available from: https://iris.who.int/handle/10665/347370.
6. Santero M, Ortiz Sequeira R, Cruz Paixao M, Muñoz Martinez M, Mazorra Roig P, Chantada G, et al. Childhood cancer survival in low- and middle-income countries and the Global South: emerging evidence and critical gaps from a scoping review of observational studies. Authorea [Preprint]. June 19, 2025. Available from: https://www.authorea.com/doi/full/10.22541/au.175034169.99781789/v1.
7. Li T, Kong X, He D. Epidemiology and clinical features of childhood malignant solid tumors in a single center in southwest China over 24 years. BMC Pediatr 2025;25(1):12. doi:10.1186/s12887-024-05360-3
8. Wu Y, Deng Y, Wei B, Xiang D, Hu J, Zhao P, et al. Global, regional, and national childhood cancer burden, 1990-2019: an analysis based on the Global Burden of Disease Study 2019. J Adv Res 2022;40:233-47. doi:10.1016/j.jare.2022.06.001
9. Jorjani G, Roshandel G, Taherian MR, Mirbehbahani N, Moaddabshoar L, Ahmadi A, et al. Epidemiology and geographical patterns of common childhood cancers in Iran: evidence from the National Cancer Registry. Cancer Epidemiol 2024;93:102685. doi:10.1016/j.canep.2024.102685
10. Shabani M, Saeedi Moghaddam S, Ataeinia B, Rezaei N, Mohebi F, Mohajer B, et al. Trends of national and subnational incidence of childhood cancer groups in Iran: 1990-2016. Front Oncol 2019;9:1428. doi:10.3389/fonc.2019.01428
11. Jadali F, Aghayan Golkashani H, Habibi G, Rouzrokh M, Abdollah Gorji F, Dini F, et al. Survey on childhood solid malignant tumors in cases admitted to mofid pediatric hospital from 1996-2010: a single-center study. Iran J Cancer Prev 2012;5(2):93-104.
12. Zlotnik H. World Population Prospects: The 2006 Revision, Vol. I, Comprehensive Tables (United Nations Publication, Sales No. E.07.XIII.2). United Nations, Department of Economic and Social Affairs, Population Division; 2007.
13. Management and Planning Organization of Tehran. Tehran (Iran: Province) – Statistics -- Yearbooks. Statistical Center of Iran, Management and Planning Organization of Tehran; 1996-2022.
14. Ahmad OB, Boschi-Pinto C, Lopez AD, Murray CJ, Lozano R, Inoue M. Age Standardization of Rates: A New WHO Standard. Geneva: World Health Organization; 2001. p. 1-14.
15. Coffin CM, Dehner LP, O'Shea PA. Pediatric Soft Tissue Tumors: A Clinical, Pathological, and Therapeutic Approach. Baltimore: Lippincott Williams & Wilkins; 1997.
16. Park JR, Eggert A, Caron H. Neuroblastoma: biology, prognosis, and treatment. Pediatr Clin North Am 2008;55(1):97-120. doi:10.1016/j.pcl.2007.10.014
17. Pickles JC, Hawkins C, Pietsch T, Jacques TS. CNS embryonal tumours: WHO 2016 and beyond. Neuropathol Appl Neurobiol 2018;44(2):151-62. doi:10.1111/nan.12443
18. Chang ET, Adami HO. The enigmatic epidemiology of nasopharyngeal carcinoma. Cancer Epidemiol Biomarkers Prev 2006;15(10):1765-77. doi:10.1158/1055-9965.Epi-06-0353
19. Ottaviani G, Jaffe N. The epidemiology of osteosarcoma. Cancer Treat Res 2009;152:3-13. doi:10.1007/978-1-4419-0284-9_1
20. Cheng W, Sun X, Yang S, Kang K, Wang L, Han C, et al. Epidemiologic trends for pediatric Hodgkin and non-Hodgkin lymphomas: a US population-based study. Ann Hematol 2025;104(6):3299-307. doi:10.1007/s00277-025-06445-4
21. Frazier AL, Amatruda JF. Pediatric Germ Cell Tumors: Biology Treatment Survivorship. Berlin: Springer; 2013. p. 135.
22. Ries LA, Smith MA, Gurney JG, Linet M, Tamra T, Young JL, et al. Cancer Incidence and Survival Among Children and Adolescents: United States SEER Program, 1975-1995. Maryland: National Cancer Institute; 1999. p. 179.
23. Weil BR, Billmire DF. Management of germ cell tumors in pediatric patients. Surg Oncol Clin N Am 2021;30(2):325-38. doi:10.1016/j.soc.2020.11.011
24. Siegel RL, Miller KD, Wagle NS, Jemal A. Cancer statistics, 2023. CA Cancer J Clin 2023;73(1):17-48. doi:10.3322/caac.21763
25. Steliarova-Foucher E, Fidler MM, Colombet M, Lacour B, Kaatsch P, Piñeros M, et al. Changing geographical patterns and trends in cancer incidence in children and adolescents in Europe, 1991-2010 (Automated Childhood Cancer Information System): a population-based study. Lancet Oncol 2018;19(9):1159-69. doi:10.1016/s1470-2045(18)30423-6
26. Linet MS, Brown LM, Mbulaiteye SM, Check D, Ostroumova E, Landgren A, et al. International long-term trends and recent patterns in the incidence of leukemias and lymphomas among children and adolescents ages 0-19 years. Int J Cancer 2016;138(8):1862-74. doi:10.1002/ijc.29924
27. Kreis C, Héritier H, Scheinemann K, Hengartner H, de Hoogh K, Röösli M, et al. Childhood cancer and traffic-related air pollution in Switzerland: a nationwide census-based cohort study. Environ Int 2022;166:107380. doi:10.1016/j.envint.2022.107380
28. Ostrom QT, Gittleman H, Fulop J, Liu M, Blanda R, Kromer C, et al. CBTRUS statistical report: primary brain and central nervous system tumors diagnosed in the United States in 2008-2012. Neuro Oncol 2015;17(Sup pl 4): iv1-62. doi:10.1093/neuonc/nov189
29. Ward E, DeSantis C, Robbins A, Kohler B, Jemal A. Childhood and adolescent cancer statistics, 2014. CA Cancer J Clin 2014;64(2):83-103. doi:10.3322/caac.21219
30. Neugut AI, Sackstein P, Hillyer GC, Jacobson JS, Bruce J, Lassman AB, et al. Magnetic resonance imaging-based screening for asymptomatic brain tumors: a review. Oncologist 2019;24(3):375-84. doi:10.1634/theoncologist.2018-0177
31. McKean-Cowdin R, Calle EE, Peters JM, Henley J, Hannan L, Thurston GD, et al. Ambient air pollution and brain cancer mortality. Cancer Causes Control 2009;20(9):1645-51. doi:10.1007/s10552-009-9412-1
32. Campbell K, Siegel DA, Umaretiya PJ, Dai S, Heczey A,

Lupo PJ, et al. A comprehensive analysis of neuroblastoma incidence, survival, and racial and ethnic disparities from 2001 to 2019. Pediatr Blood Cancer 2024; 71(1): e30732. doi:10.1002/pbc.30732
33. Bray F, Ferlay J, Soerjomataram I, Siegel RL, Torre LA, Jemal A. Global cancer statistics 2018: GLOBOCAN estimates of incidence and mortality worldwide for 36 cancers in 185 countries. CA Cancer J Clin 2018;68(6):394-424. doi:10.3322/caac.21492
34. Qin R, Xu W, Xu H, Qin Q, Liang X, Lai X, et al. The burden of common neurological disorders in Asia: insights from the Global Burden of Disease Study (1990-2021). J Neurol 2025;272(5):333. doi:10.1007/s00415-025-13074-4
35. Yue C, Zhang Q, Sun F, Pan Q. Global, regional and national burden of neuroblastoma and other peripheral nervous system tumors, 1990 to 2021 and predictions to 2035: visualizing epidemiological characteristics based on GBD 2021. Neoplasia 2025;60:101122. doi:10.1016/j.neo.2025.101122
36. Taghizadeh F, Mokhtarani B, Rahmanian N. Air pollution in Iran: the current status and potential solutions. Environ Monit Assess 2023;195(6):737. doi:10.1007/s10661-023-11296-5
37. Talkhabi H, Jafarpour Ghalehteimouri K, Toulabi Nejad M. Integrating Tehran metropolitan air pollution into the current transport system and sprawl growth: an emphasis on urban performance and accessibility. Discov Cities 2024;1(1):6. doi:10.1007/s44327-024-00008-4
38. Izquierdo JN, Schoenbach VJ. The potential and limitations of data from population-based state cancer registries. Am J Public Health 2000;90(5):695-8. doi:10.2105/ajph.90.5.695